Canadian Science Publishing | Biochemistry and Cell Biology

# Genes responsive to rapamycin and serum deprivation are clustered on chromosomes and undergo re-organization within local chromatin environments.



| | |
|---|---|
| Journal: | *Biochemistry and Cell Biology* |
| Manuscript ID | bcb-2019-0096.R1 |
| Manuscript Type: | Article |
| Date Submitted by the Author: | 07-Jun-2019 |
| Complete List of Authors: | Belak, Zachery; University of Saskatchewan, Food and Bioproduct Sciences<br>Pickering, Joshua ; University of Saskatchewan, Biochemistry, Microbiology and Immunology<br>Gillespie, Zoe; University of Saskatchewan, Biochemistry, Microbiology and Immunology<br>Audette, Gerald; York University, Chemistry<br>Eramian, Mark; University of Saskatchewan, Computer Science<br>Mitchell, Jennifer; University of Toronto, Cell and Systems Biology<br>Bridger, Joanna; Brunel University<br>Kusalik, Anthony; University of Saskatchewan, Computer Science<br>Eskiw, Christopher; University of Saskatchewan, Food and Bioproduct Sciences |
| Keyword: | Chromosome territory, long range interaction, gene expression, rapamycin, quiescence |
| Is the invited manuscript for consideration in a Special Issue? : | Not applicable (regular submission) |
| | |

# Genes responsive to rapamycin and serum deprivation are clustered on chromosomes and undergo re-organization within local chromatin environments.

**Authors**: Zachery R. Belak*[1], Joshua. A. Pickering[$1], Zoe. E. Gillespie[$], Gerald Audette[%], Mark Eramian[#], Jennifer. A. Mitchell[§], Joanna. M. Bridger[Ψ], Anthony Kusalik[#] and Christopher H. Eskiw*[$]

**Affiliations**: $: Department of Biochemistry; University of Saskatchewan; *: Department of Food and Bioproduct Sciences, #: Department of Computer Science, University of Saskatchewan; %: Department of Chemistry, York University; §: Department of Cell and Systems Biology, University of Toronto; Ψ: Department of Life Sciences, Brunel University.

[1] : These authors contributed equally to this manuscript

Corresponding author:

Christopher H. Eskiw; c.eskiw@usask.ca

Abstract:

We previously demonstrated that genome reorganization, through chromosome territory repositioning, occurred concurrently with significant changes in gene expression in normal primary human fibroblasts treated with the drug rapamycin, or stimulated into quiescence. Although these events occurred concomitantly, it is unclear how specific changes in gene expression relate to reorganization of the genome at higher resolution. Using computational analyses, genome organization assays and microscopy, the relationship between chromosome territory positioning and gene expression was investigated. We determined that despite relocation of chromosome territories, there was no substantial bias in the proportion of genes changing expression on any one chromosome, including chromosomes 10 and 18. Computational analyses identified that clusters of serum deprivation and rapamycin-responsive genes along the linear extent of chromosomes. Chromosome conformation capture (3C) analysis demonstrated the strengthening or loss of specific long-range chromatin interactions in response to rapamycin and quiescence induction, including a cluster of genes containing *Interleukin-8* and several chemokine genes on chromosome 4. We further observed that the *LIF* gene, which is highly induced upon rapamycin treatment, strengthened interactions with up- and down-stream intergenic regions. Our findings indicate that the re-positioning of chromosome territories in response to cell stimuli, this does not reflect gene expression changes occurring within physically clustered groups of genes.

**Key words:** Rapamycin, quiescence, gene expression, chromosome territory, long-range chromatin interaction.

**Background**: The genetic material in eukaryotes is organized into long linear polymers of DNA called chromosomes which provide information for cellular function (e.g. gene expression). It has now become apparent that not only is the primary sequence of DNA important for function, but also additional information, such as epigenetic marks and transcription factor binding are required. In addition, the physical organization and folding of the genome within nuclei and its ability to reorganize upon cell stimuli has been identified as important for mediating function.

The most well documented examples of genome organization influencing function are the folding of enhancer regions to form contacts with promoters. For example, expression of the *globin* gene cluster (located on chromosome 7 in mice and chromosome 11 in humans) in developing erythroblasts is regulated by an array of up-stream enhancers, called the locus control region (LCR) **(Carter et al. 2002; Mitchell et al. 2012; Schoenfelder et al. 2010b)**. The LCR, located ~50 kB away, is folded to form a long-range chromatin interaction with the *globin* promoters **(Carter et al. 2002; Tolhuis et al. 2002)**. In mice, disruption of this interaction reduces the expression of these *globin* genes to ~5% of their normal levels, leading to severe anaemia and embryonic lethality. The globin gene locus is structured head-to-tail, with specific globin genes only being transcribed at defined stages of development. The *ε–globin* gene, only transcribed in embryogenesis, is in close physical proximity to the LCR only at this stage of development. At day 14.5 of embryogenesis, when haematopoiesis transitions from the liver to the bone marrow, the LCR is in physical proximity to the *β–major globin* gene, driving its expression **(Carter et al. 2002; Siatecka and Bieker 2011; Tewari et al. 1998)**.

The development of chromosome conformation capture (3C) **(Dekker et al. 2002)** and its derivatives **(Dostie et al. 2007; Fraser et al. 2012; Lieberman-Aiden et al. 2009; Schoenfelder et al. 2010b)**, has allowed for the identification of interactions essential for several biological processes. 3C, in combination with computer modelling were used to identify the interaction of two enhancer elements, SRR107 and SRR111, with the *Sox2* gene (located >100kb up-stream) in mouse embryonic stem cells **(Zhou et al. 2014)**. CRISPR-mediated deletion of these enhancers demonstrated a significant decrease in *Sox2* mRNA and protein production, leading to impaired neural ectoderm formation, thus demonstrating the importance of these long-range chromatin interactions. Hi-C and other genome-wide chromatin conformation assays have characterized folding patterns in a variety of cell types from a number of model organisms, including *Drosophila melanogaster* **(Sexton et al. 2009; Sexton et al. 2012)**, *Mus musculus* and several human cell lines. These assays have identified locally folded domains of chromatin ranging in size between 100,000-1,000,000 base pairs, called topologically associated domains (TADs) **(Lieberman-Aiden et al. 2009)**. It is postulated that TADs containing like-regulated genes and their associated

regulatory elements are spatially organized into functional local environments involved in modulating gene expression. It is also hypothesized that the ability of genes to interact with other genes/genomic elements outside the TAD in which they reside is decreased. Furthermore, it is purported that TADs are evolutionarily maintained and that the organization of genes and regulatory element structures within TADs are highly conserved between species, but how these TADs are linked or organized into chromosomes is divergent **(Dixon et al. 2012; Pevzner and Tesler 2003)**.

Chromatin in live cells is far from static. Dundr and colleagues demonstrated that an artificially tagged *U2* gene locus can be rapidly recruited to a positionally stable Cajal body **(Dundr et al. 2007)**. This movement was found to be directional and dependant on nuclear actin polymerization, and therefore, is an active process. The dynamic nature of the genome is not limited to small domains. Upon serum starvation of human normal dermal fibroblasts, entire chromosomes re-position within the nuclear volume. These changes are rapid, occurring within 15 minutes of stimulation and are also driven by actin and nuclear myosin **(Mehta et al. 2011)**, further demonstrating the active nature of chromatin and chromosomes. However, it still remains unclear what impact the re-positioning of chromosome territories has and if this re-positioning indicates a re-organization of TADs to support changes in gene expression.

We previously reported that treatment of normal dermal fibroblasts with rapamycin or serum deprivation (which induced quiescence) increased population doubling times, changed gene expression profiles, and caused re-positioning of chromosome territories **(Gillespie et al. 2015)**. However, it is unclear if chromosome territory repositioning biases specific chromosomes to changes in gene expression. We observed that although chromosomes 10 and 18 significantly repositioned in nuclei in response to decreased serum levels and rapamycin, this did not bias these chromosomes to a greater number of genes changing expression. However, we did observe specific clusters of genes changing expression along the linear length of chromosomes. To determine how pervasive this clustering was genome-wide, we developed a linear locality clustering algorithm to identify proximal regions of the genome that were up- or down-regulated

in response to treatment under both conditions. Although activation or repression of clusters was observed for both rapamycin and serum depletion, these clusters were distinct between the two conditions. Further analyses demonstrated that these clusters of genes significantly overlapped with topologically associated domains (TADs) **(Dixon et al. 2012)**. We utilized 3C assays to determine if changes in expression levels resulted in reorganization of chromatin within specific gene clusters changing expression in response to stimuli. Specifically, we probed a region of chromosome 4 containing the *Interleukin 8 (Il-8) (*also known as *C-X-C motif chemokine ligand (CXCL)-8)* gene as well as several other genes up-regulated by rapamycin in the same cluster and observed significant changes in interaction frequency. In addition, 3C assays demonstrated that the *leukaemia inducible factor (LIF)* gene, which was significantly up-regulated in response to rapamycin, formed stronger interactions both up- and down-stream of the coding gene, which may represent putative enhancer elements. Although indicative of genome reorganization, which is associated with changes in gene expression, chromosome territory re-positioning is not sufficient to predict which chromosomes/or genes changing expression in response to stimuli. The mechanistic link between chromosome re-positioning and changes in the local folding environment of specific gene clusters (likely within specific TADs) responsive to rapamycin and serum deprivation remains to be identified.



**Results**:

**Significant re-positioning of specific chromosomes does not predict changes in transcript profiles in primary fibroblasts.**

Previous observations (Mehta et al. 2010) demonstrated that several chromosomes are re-positioned within the nuclear volume in response to serum deprivation, with chromosomes 10 and 18 exhibiting the most significant repositioning. Furthermore, chromosomes 10 and 18 are mis-localized in the premature aging disease Hutchinson Gilford Progeria Syndrome, indicating a link possible link between this disease and genome organization(Mehta et al. 2011). In addition, we have reported (Gillespie et al. 2015) that chromosomes 10 and 18 are repositioned within the nuclear volume in response to rapamycin to very similar positioning to that of quiescent fibroblasts, concomitantly with changes in cell population doubling times and alteration in gene

expression profiles. This change in positioning of chromosome 10 and 18 in response to stimuli provide an excellent model to study the relationship between chromosome re-positioning and impacts on gene expression. In addition to our observations, numerous studies demonstrate alteration of genome organization corresponds to significant changes in gene expression **(Carter et al. 2002; Chambeyron et al. 2005; Cope et al. 2010; Dixon et al. 2012; Schoenfelder et al. 2010b)**. We therefore hypothesized that as both chromosomes 10 and 18 experienced a significant change in nuclear positioning, that a higher proportion of genes with altered expression would be located on these chromosomes. Chromosome 10 encodes 4.3% of all the genes in the genome, whereas chromosome 18 encodes 1.0%. Therefore we hypothesized that out of all genes observed changing expression in response to rapamycin ~4.3% would be located on chromosome 10 and ~1% would be located on chromosome 18.. Rapamycin induced a >5-fold change in expression of 538 genes **(Gillespie et al. 2015),** 20/538 (3.7%) of these genes were located on chromosome 10 and 3/538 (0.6%) were located on chromosome 18 **(Figure 1)**. The genes responsive to serum depletion were substantially different from those responsive to rapamycin (see (Gillespie et al., 2015) for full analysis) and, therefore, represent different biological pathways. However, we observed a similar distribution of genes changing expression; 28/755 (3.7%) were located on chromosome 10 and 4/755 (0.5%) were located on chromosome 18.

To determine if there were biases to any one chromosome in terms of numbers of genes either up- or down-regulated, we examined the proportion of genes changing expression on each chromosome. In order to analyze this bias, we compared the proportion of genes present on each chromosome to the proportion of genes identified as changing expression on that chromosome. The greatest difference between proportion of genes and proportion of genes changing expression was observed for chromosome 16 after treatment with rapamycin. Since chromosome 16 contains 3.1% of all genes in the chromosome, we would expect, if a random distribution of genes were responsive, that only 3.1% of all genes changing expression in response to rapamycin. However, we observed that 7.8% of genes down-regulated in response to rapamycin were located here. Similarly, while chromosome 17 encodes 4.1% of all genes in

the genome we observed that it 8.6% of genes down-regulated under quiescent conditions were localized to this chromosome **(Supplemental Fig 1)**. These data indicate there can be substantial differences between the number of genes encoded by a given chromosome and the number of genes changing expression on that chromosome.

To further confirm these observations, we compared the proportion of genes changing expression under a given treatment condition using z-scores. The z-score is the number of standard deviations the proportion of genes changing expression on a given chromosome differs from the average proportion of genes with altered expression across all chromosomes. Positive z-scores indicate chromosomes that have a higher number of genes changing expression than the average across all chromosomes while negative values represent chromosomes with fewer genes changing expression (**Supplemental Figure 2**). Z-scores were calculated independently for each of the up-regulated and down-regulated gene lists and for each treatment condition. In this case the p-value does not indicate a confidence interval nor a probability but represents a mathematical transformations used to compare the percentile of the proportion of genes changing on each chromosome to the average across all chromosomes. This facilitates the identification of chromosomes with substantial bias in terms of number of genes up or down-regulated. For example, in serum deprived fibroblasts, chromosome 17 had a z-score of -2.27, indicating that the proportion of up-regulated genes found on chromosome 17 was 2.27 standard deviations lower than the average proportion of genes up-regulated across all chromosomes. This corresponds to a p-value of 0.02 indicating that chromosome 17 is in the bottom 5% of chromosomes in terms of proportion of genes up-regulated by serum deprivation. Chromosome 17 also had a z-score of 2.35 with a corresponding p-value of 0.02 for down-regulated genes indicating an over-representation of genes being repressed on that chromosome relative to the average. In addition to chromosome 17, we observed that chromosome 16 had a z-score of 2.20 with an associated p-value 0.03 in response to rapamycin, indicating a proportionally high number of genes were down-regulated on this chromosome. Other than these exceptions, no chromosome shows more than 2.35 standard deviations when compared to the proportion of genes on each chromosome, with most falling within +/- 1 standard deviation. We interpret these data to indicate that there is a relatively equal distribution of genes on each chromosome

undergoing transcriptional changes in response to rapamycin and quiescence induction, regardless of re-positioning of chromosomes.

To further test bias in the number of genes changing expression versus chromosome positioning, we performed chromosome painting for chromosome 4 following rapamycin treatment in dermal fibroblasts. Chromosome 4 encodes a cluster of significantly up-regulated genes (including *Il-8* gene as well as several *CXCL* genes) involved with cytokine-cytokine receptor pathway (Gillespie et al., 2015), many of which are located within a 1Mb region of this chromosome. We hypothesized that if an entire chromosome is moved in response to transcriptional requirements, this would be a potential candidate. Using chromosome painting and erosion analyses **(Gillespie et al. 2015; Mehta et al. 2011),** we observed a subtle but significant shift of this chromosome from an intermediate to a peripheral nuclear position in response to quiescence; however, no significant shift in chromosome 4 position was observed in response to rapamycin (**Figure 2**). While some chromosomes are re-positioned under different stimuli, the link between cell stimuli, chromosome re-positioning and genome function remains to be defined. Nevertheless, the lack of re-positioning of chromosome 4 does not discount the possibility that smaller changes in the local nuclear environment (as other chromosomes are moving) or sub-territory re-organization is occurring.

Previous observations indicate that loci can relocate within the nuclear volume in response to stimuli **(Branco et al. 2008; Dundr et al. 2007)**. To determine if the observed change in transcriptional output from this region on chromosome 4 resulted in a change in nuclear location, we performed DNA FISH using bacterial artificial chromosome (BAC) probes (Rp11-121H14) and quantified the location of the alleles using erosion analysis (**Supplemental Figure 3**). We observed that quiescence induced a repositioning of this loci from an intermediate position within the nucleus to the centre compared to proliferative cells. Unfortunately, we were unable to obtain data from for dual labelling with chromosome paints and individual BAC probes to determine if stimuli caused looping of this region outside of the chromosome territory. The positioning of this region in rapamycin treated cells remained relatively constant within the volume although this region contained genes with the largest differential expression response to rapamycin. As we did

not observe substantial bias in the proportion of genes changing expression on chromosomes 10 or 18, and given a lack of observed large variations with any other chromosome, in addition to no significant change in the positioning of chromosome 4 in response to rapamycin, we did not further pursue positioning of other chromosomes via FISH.

**Groups of genes in proximity along chromosomes change expression in response to rapamycin and serum depletion**.

Although we did not observe any one chromosome exhibiting biases in the number of genes changing expression, we did observe that groups of genes in proximity along the length of chromosomes were responsive to rapamycin. For example, several genes within a 1 MB region of chromosome 4 (positions 74,606,000-75,610,000) significantly increased expression following rapamycin treatment, including: *IL-8 (CXCL8)*, *CXCL6*, *CXCL1*, *CXCL3*, *CXCL2*, *EREG*, *AREG* and *AREGB* (**Figure 3**). We further observed that in a 1 MB region of chromosome 2 (position 110,500,000-111,500,000), *RGPD5*, *LIMS3* and *RGPD6* genes were significantly up-regulated (**Supplemental Figure 4A-C**). Although *Mall,* another gene within this region, did not reach our ≥5-fold cutoff for significance, it was up-regulated 2.28-fold. In addition, rapamycin induced the increased expression of a cluster of genes located on chromosome 19 (position 43,250,000-44,500,000), several of which met our criteria for significance in addition to several that changed expression ≥2-fold (**Supplemental Figure 5A-C**). These belong to the *pregnancy specific glycoprotein (PSG)* gene family and encode members of the immunoglobulin superfamily **(Teglund et al. 1994)**. Although the biological impact of the up-regulation of some of these gene clusters remains to be elucidated, our observations indicate that specific clusters of genes along the length of chromosomes are responsive to rapamycin.

Genes responsive to low serum levels were also clustered along the length of chromosomes. In quiescent fibroblasts, 38/755 (5.0%) of the genes changing expression were located on chromosome 17 (**Supplemental Figure 1**). Of these genes, 13 (located at position 39,182,000-39,222,000) are members of the *keratin associated protein (KRTAP)* family, and constitute a subset of a larger cluster of *KRTAP* genes linked with hair development **(Fujikawa et al. 2012)**.

Two other *KRTAP* gene clusters are present in the human genome, located on chromosomes 11 and 21; however, the transcript profiles of these genes were not significantly altered. **(Perez 2011)**.

Based on our observation that clusters of genes were responding to rapamycin and serum depletion, we performed genome-wide analyses to determine the overall extent to which genes with altered transcript profiles are physically clustered. Our aim was not to demonstrate that genes are physically clustered on chromosomes, but to demonstrate that these clusters become active or inactive in response to rapamycin and serum depletion. We analysed the degree of up- or down-regulated gene clustering by sequential gene processing using a linear locality clustering algorithm developed in-house. Utilizing a sliding window of different sizes, we defined a cluster as two or more gene transcription start sites located within a single window. To avoid artificial inflation of the number of clusters, each gene was restricted to a single cluster assignment. Very few transcriptionally responsive clusters were observed using small window sizes (1 Kb to 20 Kb) in either rapamycin-treated or quiescent fibroblasts (**Supplemental Table 1**). At a 50 Kb window size, 15.42% (66/431; 27 individual clusters) of up-regulated genes and 26.01% (84/324; 34 individual clusters) down-regulated genes following quiescence induction were present in clusters, while 13.3% (56/422; 21 individual clusters) of up-regulated and 12.93% (15/116; 7 individual clusters) down-regulated genes responsive to rapamycin were also found in clusters. When the window size was expanded to 1 MB, 45.9% (198/431; 76 individual clusters) up-regulated genes and 53.4% (173/324; 57 individual clusters) of down-regulated genes exhibited clustering in quiescent fibroblasts. Similarly, 42.7% (180/422; 15 individual clusters) of the rapamycin up-regulated genes and 31.9% (37/116; 65 individual clusters) of the down-regulated genes exhibited clustering at this window size (**Supplemental Figure 6**). At a window size of 5 MB, ~80% of both up-regulated and down-regulated genes under quiescence induction and rapamycin treatment were present in clusters. We generated random gene lists (containing an equivalent number of genes) and compared these to our datasets to empirically determine if clustering was statistically significant. All window sizes demonstrated significant clustering of genes in both quiescent (**Table 1A**) and rapamycin-treated (**Table 1B**) fibroblasts with the

exception of the 2 MB window in the rapamycin up-regulated genes. For each window size, the total number of genes in clusters, the total percent of genes changing expression in clusters, and the average number of genes in each cluster in quiescent and rapamycin treated cells are given in **Supplemental Tables 2A-C**. Comparison and statistical analyses demonstrated that specific regions of the genome are activated/repressed in response to rapamycin and serum depletion exposure.

Table 1A

| Window Size | QUI ≥5-fold over-expressed | p-value | QUI ≤5-fold under-expressed | p-value |
|---|---|---|---|---|
| **1 kB** | 5 | 2.89E-21 | 5 | 3.02E-27 |
| **2 kB** | 5 | 2.92E-17 | 7 | 2.38E-27 |
| **5 kB** | 10 | 3.23E-18 | 13 | 6.23E-25 |
| **10 kB** | 14 | 4.17E-19 | 18 | 1.41E-25 |
| **20 kB** | 18 | 7.21E-17 | 24 | 4.90E-26 |
| **50 kB** | 27 | 1.05E-16 | 34 | 1.14E-25 |
| **100 kB** | 35 | 1.70E-16 | 38 | 4.87E-23 |
| **200 kB** | 51 | 1.24E-16 | 44 | 7.68E-21 |
| **500 kB** | 64 | 1.04E-13 | 50 | 6.23E-17 |
| **1 Mb** | 76 | 9.61E-11 | 57 | 4.86E-15 |
| **2 Mb** | 88 | 8.30E-03 | 68 | 1.94E-09 |
| **5 Mb** | 94 | 1.80E-04 | 62 | 1.66E-12 |

Table 1B

| Window Size | RAP ≥5-fold over-expressed | p-value | RAP ≤5-fold under-expressed | p-value |
|---|---|---|---|---|
| **1 kB** | 3 | 3.12E-20 | 2 | 1.34E-19 |
| **2 kB** | 6 | 4.63E-26 | 3 | 5.46E-23 |
| **5 kB** | 9 | 1.23E-22 | 5 | 3.02E-27 |
| **10 kB** | 14 | 1.17E-22 | 5 | 5.12E-23 |
| **20 kB** | 16 | 1.43E-20 | 6 | 1.49E-23 |
| **50 kB** | 21 | 2.52E-18 | 7 | 1.24E-19 |
| **100 kB** | 33 | 7.32E-19 | 8 | 5.88E-20 |

| | | | | |
|---|---|---|---|---|
| **200 kB** | 40 | 1.44E-16 | 9 | 7.68E-19 |
| **500 kB** | 52 | 6.77E-10 | 14 | 6.33E-18 |
| **1 Mb** | 65 | 2.63E-03 | 15 | 5.45E-16 |
| **2 Mb** | 82* | 8.63E-01 | 20 | 6.81E-16 |
| **5 Mb** | 88 | 3.31E-07 | 23 | 7.80E-09 |

**Table 1: Genes responding to quiescence induction and rapamycin are physically clustered in the human genome.** The number of gene clusters that changed transcript abundance in quiescence induced (A) or following rapamycin treatment (B) as detected by linear locality clustering using various window sizes. The number of clusters was compared against locality clustering performed on 20 randomly generated lists of genes to empirically generate p-values. * represents statistically insignificant clustering.



**Clusters of responsive genes overlap with topologically associated domains**:

Several seminal findings have indicated that organization and folding of the genome within the nuclear volume is essential for the regulation of gene expression in development and disease **(Cope et al. 2010; Fraser and Bickmore 2007; Lee et al. 2005; Osborne et al. 2007; Phillips-Cremins et al. 2013; Zhang et al. 2012; Zullo et al. 2012)**. The genome is further theorized to fold sub-chromosomal regions into compartmentalized local environments, called topologically associated domains (TADs), which are proposed to be evolutionarily conserved and limit the inappropriate activation/repression of genes located in adjacent genomic regions **(Dixon et al. 2012; Lieberman-Aiden et al. 2009)**. We therefore tested if the clusters of genes identified by linear locality clustering overlapped with previously identified boundaries for specific TADs. Clusters identified within the 1 MB window were compared with the locations of TADs previously identified through Hi-C and CCCTC-binding factor (CTCF) ChIP-seq in IMR90 fibroblasts **(Dixon et al. 2012)**, which are hypothesized to be conserved in all human cell types. In response to rapamycin, 33/65 of our up-regulated clusters identified in 2DD cells using the 1 MB sliding window (50.8%) and 8/15 (53.3%) down-regulated clusters were contained within individual TADs identified within IMR90 cells. Other clusters were either located partially in one TAD and the adjacent un-organized chromatin or spanned multiple TADs.

Rapamycin treatment of 2DD primary fibroblasts induced up-regulation of genes *Il-8*, *CXCL-1*, *CXCL-3*, and *CXCL-2,* all of which are contained within a putative TAD located at position 74,160,001-75,240,000 **(Dixon et al. 2012), (Supplemental Figure 7)**. Rapamycin also caused the up-regulation of *epiregulin* (*EREG)* (75,230,860-75,254,468), located at a TAD boundary and partially overlapping with the unorganized chromatin domain, with the following TAD containing *amphiregulin* (*AREG)*. *IL-8*, *CXCL-1*, *CXCL-3*, and *CXCL-2* are functionally related and are associated with the same KEGG pathway term (cytokine-cytokine receptor interaction). Furthermore, we previously reported that these genes are regulated by the signal transduction activator of transcription (STAT) 5A/B transcription factor **(Gillespie et al. 2015)**. Given that several clusters of genes changing expression overlapped with putative TADs, including the cluster containing the *Il-8* gene, we hypothesized that these regions may reorganize upon quiescence induction or rapamycin treatment, bringing together or disrupting physical interactions between specific genes within 3D space, concomitantly with changes in gene expression. To test this hypothesis, we performed chromosome conformation capture (3C) (**Figure 4**) on proliferative, quiescence-induced and rapamycin-treated 2DD fibroblasts to determine if the TAD containing *Il-8* was undergoing re-organization. Using primers flanking HindIII restriction enzyme sites, we examined *Il-8* interactions with other genes contained within this TAD and normalized this against a known interaction between adjacent restriction fragments. In the absence of specific interactions, interaction strength (defined as the relative abundance of detectable interactions) decreases as a function of genomic distance between any two points. Therefore, we first determined the decrease in interaction strength with distance from the *Il-8* gene. Use qPCR, we detected strong interaction between *Il-8* and a non-coding region of chromosome 4 located 6.4 Kb downstream (**Supplemental Table 3A and B**). We noted that the strength of this interaction was altered after rapamycin treatment and quiescence induction. There was a 6.4-fold increase in interaction strength in quiescent samples and a 3.7-fold increase in rapamycin treated cells relative to proliferative fibroblasts, indicating that there is a change in the local folding pattern even at this short range. However, interrogation of a site 16 Kb downstream showed no detectable interaction, indicating the formation of ligation products occurs at an extremely low frequency

at this genomic distance. We interpreted this decrease to undetectable interactions as an indication that the probability of interactions forming due to random chromatin dynamics, and not biological process, was extremely low 16 Kb downstream of *Il-8*. We further interpreted this as any interaction that were detected beyond this linear distance was due to biological processes, such as transcription factor binding or sharing of resources at transcription factories (Eskiw and Fraser 2011; Eskiw et al. 2008; Iborra et al. 1996; Pombo et al. 2000; Schoenfelder et al. 2010b), actively bringing loci together in the nuclear volume to facilitate interactions.

Following the initial interaction frequency based on linear distance, we probed 3C libraries for interactions between specific genes on chromosome 4 within the region of 74,000,000-75,000,000 bp (**Figure 4**). We observed changes in interaction strength for several gene pairs in response to rapamycin and serum depletion. *Il-8* and *CXCL-1,* located 128.8Kb apart, demonstrated interaction strengths similar in proliferative and quiescence cells; however, this interaction strength increased 10.6-fold in rapamycin-treated cells. This increase in interaction strength corresponds to a 5.9-fold increase in *CXCL-1* transcript abundance and a 24.1-fold increase in *Il-8* transcripts, as previously documented **(Gillespie et al. 2015)**. *Il-8* interacted strongly with *CXCL-3* (9.2-fold increase in transcript abundance) and the interaction was strengthened in both quiescence (2.2-fold) and rapamycin (3.3-fold) treated cells. To ensure that we were not observing artefacts as a result of using a single anchor gene, we also tested interactions between *CXCL-1* and other genes within this TAD (**Supplemental Figure 8 and Supplemental Table 4**). Rapamycin increased the strength of detectable interactions between *CXCL-1*/*CXCL-6* (2.5-fold), *CXCL-1/CXCL-3* (2.4-fold) and *CXCL-1/CXCL-2* (4.3-fold) while serum depletion altered interaction strengths 6.3-fold, 1.9-fold and -2.0-fold respectively. There were examples of interactions that were detectable but did not have significant changes; *Il-8* and *CXCL-6* (96.6 Kb) formed interactions with similar strengths in proliferative and rapamycin treated samples with a slight decrease observed in quiescent cells. Although *CXCL-2* increased transcript abundance by 5.16-fold in response to rapamycin, no interaction with *Il-8* was detected, indicating an interaction frequency too low to detect or that these genes are not transcribed in close physical proximity.

RNA-seq data analysis had previously demonstrated that *EREG* expression increased 11.3-fold in response to rapamycin and *AREG* 81.5-fold. Quiescence induction also increased *AREG* expression 5.9-fold, while having little effect on *EREG* expression. As *Il-8*, *CXCL-1*, *CXCL-3* and *CXCL-2* mapped to one TAD, while *EREG*, *AREG* and *AREGB* mapped either to an unstructured domain or to the adjacent TAD, we tested if the proposed TAD boundary did in fact prevent inter-TAD interactions. Strong interactions were detected between two adjacent fragments of the *EREG* gene (located 500 bp apart) and between *AREG* and *EREG* (**Supplemental Table 5A and B**). The later interaction increased in strength by 20-fold in quiescence and 3.3-fold in rapamycin treated cells relative to proliferative fibroblasts. However, no interactions were detected between *EREG* and *CXCL-2* in the adjacent TAD. One possibility for the observed lack of detectable interaction is that the long physical distance between *EREG* and *CXCL-2* (~300 Kb) make this interaction difficult to detect. Although we cannot exclude this, we were able to detect other interactions (such as those between *Il-8* and *CXCL-3*) at similar or larger distances; therefore, we suggest that the lack of interactions between *EREG* and *CXCL-2* is likely due to each gene belonging to separate TADs resulting in no interaction.

Both quiescence induction and rapamycin treatment resulted in the up-regulation of *KRTAP* genes. As previously noted, these genes are present as clusters. We probed the region of chromosome 17 spanning ~150 Kb containing several up-regulated *KRTAP* genes using 3C. Using the *KRTAP2-3* gene as an anchor, we identified a strong interaction between this gene and *KRTAP1-1* (~30 Kb up-stream) in proliferative, quiescent and rapamycin-treated 2DD cells (**Supplemental Figure 9 and Supplemental Table 6**). In proliferative cells, interactions between *KRTAP2-3* were identified with *KRTAP1-5* (-36Kb) and *KRTAP3-1* (-50Kb); however, these interactions were significantly strengthened under treatment conditions. Many interactions of *KRTAP2-3* with up-stream genes were either weak or undetectable in proliferative cells. However, rapamycin and quiescence induction resulted in robust detection of interactions as far as ~90 kB down-stream (with the exception of *KRTAP4-1*), indicating reorganization of this region of the genome in response to decreased serum levels and rapamycin treatment.

The *leukaemia inducible factor* (*LIF*) gene (chromosome 22) was significantly up-regulated (73-fold) in rapamycin-treated primary fibroblasts **(Gillespie et al. 2015)**. DNA FISH and subsequent erosion analysis indicates that rapamycin did not cause the redistribution of the 28-29 MB region of this chromosome (**Supplemental Figure 10**). Only serum depletion resulted in quantifiable movement of this locus away from the interior of the nucleus to the periphery although transcript abundance of this gene is similar between proliferative and serum deprived cells. Regardless of the lack of detectable change in position within the nuclear volume of the *LIF* gene in response to rapamycin, the change in transcript levels indicated that stimuli might drive the promoter of this gene to interact with enhancer/regulatory elements within the local chromatin environment. RNA-seq data demonstrate several regions of transcript in intergenic regions up- and down-stream of the *LIF* gene, indicating potential enhancer regions (**Figure 5: upper panel**). In addition, examination of datasets from the ENCODE database indicates that the region of chromosome 22 containing the *LIF* gene has several regions of histone 3 lysine 27 acetylation (H3K27ac) in seven cell types (HUVECs, NHLF, K562, GM12878, hESC, HSMM and NHEK) indicative of enhancer/regulatory elements (**Figure 5: middle panel**). Although not all cell lines demonstrated that these regions contained H3K27ac, we used this as a first approximation for the potential of regulatory elements to guide our analysis. Based on these observations, we interrogated 3C libraries to identify interactions within the vicinity of the *LIF* gene (**Figure 5: bottom panel**). Numerous potential interactions were undetectable, signifying that these are not functionally engaging the *LIF* gene in 2DD primary fibroblasts and hence are not regulatory elements. We identified an interaction with a down-stream region (5.8 Kb) that lost interaction strength in response to both rapamycin (-3.1-fold) and quiescence (-3.5-fold) compared to proliferative cells (**Supplemental Table 6A and B**). However, rapamycin treatment strengthened an interaction 7.9 Kb downstream of *LIF* (6.5-fold). A further interaction was detected 35.4Kb downstream of *LIF* (**Figure 5**); however, this was comparable in strength to the control interaction and was only slightly altered in quiescence (1.3-fold) and rapamycin (-1.8-fold) treated cells. We were able to detect interactions with the *LIF* gene and a region located 10.8 Kb upstream, which remained relatively constant (quiescence: -1.6-fold; rapamycin: 1.5-fold). However, we did observe an

increase in interaction strength (quiescence: 5.4-fold; rapamycin: 4.2-fold) 18 Kb upstream. No interactions were detected 43.4Kb upstream indicating that this region is not interacting with the *LIF* gene. However, rapamycin did induce an 11-fold increase in interaction strength with a site 63 Kb upstream with a modest 2.8-fold increase in quiescent cells. No further interactions were detected up-stream of this region (at 68 Kb and 83.4 Kb).

To investigate if the changes in interaction frequency following rapamycin treatment or quiescence induction involved putative regulatory elements marked by H3K27ac in 2DD fibroblasts, we performed ChIP for this mark in all regions probed for interactions by 3C in proliferative, quiescence-induced and rapamycin-treated 2DD cells. We observed many of these regions exhibit enrichment for H3K27ac above background; however, no significant changes in acetylation levels were observed in 2DD cells following quiescence induction and rapamycin treatment when compared to proliferative cells (data not shown). Although the *LIF* gene does change interaction frequency with the surrounding non-coding regions, chromatin within the *LIF* region may already be in an open state prior to treatment (as seen by the presence of transcripts in proliferating cells) with acetylation of distal regulatory elements not playing a major role in the up-regulation or mediation of changes in *LIF* transcription.



**Discussion**:

It is clear from several examples that chromatin movement and genome organization are related to the maintenance of gene expression patterns; however, the link between chromosome territory positioning and gene expression has not been established. We had previously reported that chromosome 10 and 18 re-position within nuclei in response to quiescence induction and rapamycin treatment of 2DD primary dermal fibroblasts, and that this re-positioning occurred concomitantly with significant changes in gene expression **(Gillespie et al. 2015)**. Given the significant re-positioning of these chromosomes, we anticipated that this would mean a larger proportion of genes changing expression due to the change in nuclear location. This was not the case; no single chromosome had a disproportionate relative number of genes changing than any other. Although several of the most highly responsive genes following rapamycin treatment were

located in a cluster on chromosome 4, this chromosome did not exhibit the same dramatic change as those seen with chromosomes 10 and 18. The individual loci encoding this region did appear to change location within the nuclear volume as identified by loci-specific DNA FISH and erosion analysis, indicating a potential looping out of this domain from the territory. These findings indicate that the movement of a chromosome is not reflective of the proportion of genes up- or down-regulated in response to stimuli. Previous findings **(Bourne et al. 2013; Croft et al. 1999; Mehta et al. 2010; Mehta et al. 2007)** conclude that the observed movement and position of chromosomes 10 and 18 in primary dermal fibroblasts are an excellent indication of changes in growth (either from proliferation to quiescence or in response to environmental queues); however, our current observations provide no indication of an effect on specific genes/biological pathways encoded on those chromosomes.

Chromosome re-positioning is indicative of genome re-organization. Although a chromosome does not change position, this does not indicate that it has not experienced a change in the local environment (as they may have new neighbours). Although the nuances of this repositioning are unclear, there must be functional consequences for the re-location of large masses of DNA/chromatin within the nuclear volume, either directly related to the genes that are moving or indirectly to change the local environment to favor the transcription of other genes. It is possible that the gene-poor nature of chromosome 18, as well as being physically small, favours this chromosome being moved within the nuclear volume more readily **(Surralles et al. 1997)**. In addition, chromosome 18 may have less necessity for long-range chromatin interactions, being re-located to favour chromatin interactions between other chromosomes.

Although no specific chromosome was enriched in up- or down-regulated genes, linear locality clustering demonstrated significant clustering of rapamycin and quiescence responsive genes along chromosomes. This clustering likely represents evolutionary processes resulting in like-regulated genes localizing in physical proximity along the length of chromosomes. The aim of our assays was not to test this hypothesis, but to indicate that specific groups of genes were changing expression in response to rapamycin or serum deprivation. While small window sizes (2Kb to

50Kb) demonstrated little evidence of clustering, at window sizes of 1 Mb, we observed that 45.9% and 53.4% of genes changing expression (up- and down-regulated respectively) are present in clusters in response to serum depletion. A previous study by Zhang and colleagues identified that cellular progression into senescence induced changes in expression of genes physically clustered along the length of chromosomes in human cells **(Zhang et al. 2003)**. However, the conclusions of Zhang and colleagues stated that there was no clustering of genes that changed expression in quiescent fibroblasts **(Zhang et al. 2003)**. The reasons for differences in these observations is currently unclear, although there could be changes due to the genotype of the cells used or methods used in identifying transcript changes. Rapamycin responsive genes also demonstrated clustering, with 42.7% and 31.9% of up- and down-regulated genes clustered. At window sizes of 5 Mb, ~80% of all genes changing expression are present in clusters. Larger window sizes of 1-5 Mb are consistent with TAD dimensions and may indicate that our observed clusters of responsive genes may represent locally folded domains of chromatin.

Hi-C data has provided a plethora of information on genome organization in response to disease and cell stimuli. Analysis of these datasets have driven several new hypotheses, including the idea that actively transcribing chromatin is compartmentalized away from transcriptionally silent chromatin, deemed the A and B compartments respectively (Dixon et al. 2012; Fortin and Hansen 2015; Lieberman-Aiden et al. 2009). As we observed significant changes in chromosome territory positioning as well as the gain or loss of interaction strength between distally located genomic regions, it is highly probable that our treatments of rapamycin and quiescence induction cause many genes to exchange between these compartments. Conversely, we did not observe many genes going from a transcriptionally silent state to an active state or *vice versa* indicating that many of the genes remained in the A compartment. Future analysis of the relationship between changes in chromosome territory positioning and the A and B compartments, using a combination of Hi-C/Hi-ChIP for specific chromatin marks, may shed light onto the significance of territory positioning with regards to biological function.

We observed that the differentially regulated *Il-8* and *CXCL* genes located on chromosome 4 were able to alter their interaction profiles in response to serum deprivation or rapamycin. Increases in interaction strength occurred concomitantly with increase in gene expression, consistent with the hypothesis that transcriptional requirements play a major role in driving genome organization **(Cook 2010; Cope et al. 2010; Fraser and Bickmore 2007; Osborne et al. 2004; Schoenfelder et al. 2010a; Xu and Cook 2008)**. However, these movements may be subtle and more consistent with sub-chromosomal domains repositioning within the nuclear environment or moderate re-organization of specific TADs to influence transcriptional changes. Rapamycin either increases or stabilizes the interaction between *Il-8/CXCL3* and *Il-8/CXCL-1*. Interactions could also be detected between *CXCL-1/CXCL-3,* although at a lower intensity. We postulate that these three genes will be found at the same transcription factory more frequently in the population; however, it remains unclear if this interaction is occurring in more cells but with the same frequency/cell or if the interaction is not occurring more often per cell due to increased transcriptional bursting. All of the genes identified are transcriptionally active in 2DD fibroblasts and their transcriptional rates are up-regulated in response to rapamycin. No genes in this analysis went from undetectable transcriptional activity to high activity or *vice versa*, thus explaining why we did not generate novel interactions or the complete loss of interactions.

The observations from chromosome 4 are consistent with our findings from the *LIF* gene on chromosome 22. *LIF* is a transcriptionally active gene in primary fibroblasts and we demonstrated that rapamycin caused a significant increase in transcript abundance by RNA-seq and qPCR. We predicated that an enhancer might be responsible for driving the expression of this gene in response to stimuli. To identify potential regulatory elements that might be promoting this increase in transcript abundance, we identified regions of the genome enriched for H3K27ac in several other cell types using ChIP-seq datasets from the ENCODE database as well as the presence of transcripts from the non-coding regions surrounding the *LIF* gene. Probing 3C libraries for these interactions demonstrated three potential sites that may facilitate the increased expression of *LIF*; one 7.9 kB downstream and two upstream, 18 kB and 63 kB. The interactions at 7.9 kB downstream and 63 kB upstream are likely candidates as there is a

significant increase in interaction strength concomitantly with an increase in transcript abundance. ChIP assays failed to identify changes in H3K27ac status of these putative enhancer regions indicating that these regions may already be primed as *LIF* expression is present at basal levels in proliferating fibroblasts and that new unutilized enhancers within this region are not activated. Although we did not observe changes in the epigenetic status of these regions, we did observe changes in the interaction strengths at specific sites, indicating that the increased expression of *LIF* in response to rapamycin likely occurs concomitantly with re-structuring of the local chromatin environment.

**Conclusions**:

From the outlined experimentation and observations, we conclude that large-scale movement of specific chromosomes within the nuclear volume does not bias any one chromosome to changes in gene expression to a greater or lesser extent than any other chromosome. We did observe that rapamycin and quiescence induction resulted in the activation or repression of clusters of genes on chromosomes, domains that are consistent in size with predicted TADs. Although the functional consequence of chromosome re-positioning remains unclear, we conclude that strengthening or weakening of specific long-range interactions within these local domains as a result of rapamycin and quiescence induction occur concomitantly with changes in gene expression.

**Materials and Methods**:

**Cell Culture**: 2DD cells were cultured as previously described **(Gillespie et al. 2015)**. Briefly, cells were grown until 70% confluent to avoid contact inhibition. To induce quiescence, cells were treated with DMEM media containing 0.5% FBS. Rapamycin treatments were performed by treating cells with 500 nM rapamycin for 5 days. Both quiescence and rapamycin treatments were maintained for 5 days.

**Linear clustering of genes along chromosomes and TAD boundary comparison**: Data for the total number of genes per chromosome was obtained for the GRch37/hg19 build at

http://jul2012.archive.ensembl.org/Homo_sapiens/Location/Chromosome for each chromosome. The total percent of genes changing expression per chromosome was calculated using the number of genes per chromosome from the website. An in-house algorithm (similar to previous methods **(Dottorini et al. 2013)**) was used to perform linear locality clustering by identifying, along the length of each chromosome, the locations of all genes that had ≥5-fold increase or decrease in transcript abundance. A cluster was defined by the presence of the transcription start site of two or more so identified genes along a linear extent of a chromosome (the window size). After determination of the clusters in one window (chromosomal segment), the position of the sliding window was advanced by a fraction of the window size, and the analysis repeated. To avoid artificial inflation of the number of clusters, each gene was restricted to being assigned to a single cluster. The analysis was performed for varying window sizes (1kB to 5MB). It determined how many genes, which had ≥5-fold increase or decrease in transcript abundance, clustered along each chromosome in response to quiescence or rapamycin treatment. To determine a p-value, the observed number of clusters was compared to the number of clusters generated by running the clustering algorithm on 20 random gene lists of the same size and applying a one-sample t-test, using previously identified methodologies **(Dottorini et al. 2013; Zhang et al. 2003)**. Comparison of TADs identified on chromosome 4 with the gene cluster located between 74,606,376-75,488,112 were performed. Briefly, the .bed file containing locations from the combined mapping of TADs in IMR90 lung fibroblasts identified by Dixon and colleagues **(Dixon et al. 2012)** was downloaded (http://yuelab.org/hi-c/download.html) and imported into SeqMonk. The positions of the TADs were marked and then compared to the location of genes identified.

**Gene distribution comparisons by z-score**: To determine if there were biases to specific chromosome containing genes changing expression in response to rapamycin and quiescence induction, the percent of genes changing expression for each chromosome was compared to the percent of genes on that chromosome in relation to the rest of the genome. The proportion of total genes located on each chromosome was calculated by dividing the number of genes on a specific chromosome vs the number of genes in the genome (([genes$^{chromosome}$]/[genes$^{genome}$]) X

100). The percent of genes changing expression for a specific chromosome was calculated by dividing the number of genes identified to change expression on a specific chromosome divided by the total number of genes changing expression. This was repeated for the all genes changing expression, up-regulated genes alone or down-regulated genes alone. z-scores were calculated using the formula Z= (X-sample mean)/(standard deviation). P-values were obtained from z-score tables.

**Chromosome Painting, BAC probe FISH and Erosion Analysis**: For chromosome painting and BAC probe FISH, proliferative, quiescence-induced and rapamycin-treated cells were grown on coverslips in 6-well dishes and fixed with 3 mL 3:1 methanol: acetic acid (4$^{o}$C). Coverslips were incubated at 4$^{o}$C for 1h. Methanol:acetic acid was exchanged 3 more times with 10 minute incubations at 4$^{o}$C. Coverslips could be stored indefinitely at 4$^{o}$C in fixative. To prepare cells for chromosome painting or BAC probe FISH by DNA FISH, coverslips were dehydrated in a graded ethanol series (70%, 90% and 3 X 100%), 10 minutes for each. Coverslips were then left to dry at room temperature for 24 hours. Coverslips were incubated in 70% formamide, 2X SSC for 2 minutes at 70$^{o}$C to denature chromatin/DNA. Coverslips were immediately plunged into ice cold 70% ethanol to form imperfect duplexes; followed by treatment in graded ethanol series as before. Coverslips were air dried, stored or immediately used for probe binding.

Probes for chromosome X were prepared as previously described **(Elcock and Bridger, 2010; Gillespie et al., 2015; Mehta et al., 2011)**. Probes were prepared by DOP-PCR from flow sorted chromosomes. The first round was used to amplify fragments of chromosomes and the second to incorporate biotinylated nucleotides. For each coverslip to be analysed, 300 ng of probe was precipitated with 3.5 μg COT-1 DNA and 3 μg of herring sperm DNA. This mixture was precipitated and resuspended in hybridization mix (50% formamide, 4X SSC, 20% dextran sulphate and 50 mM sodium phosphate). 12 μl of this mix is recommended per slide. For chromosome 4, directly labelled (Cy3) probe was donated by Cytocell/Oxford Gene Technologies. 12 μl of probe was used per coverslip.

Prior to first use, probes were denatured by heating at 75$^{o}$C, followed by 1h incubation at 37$^{o}$C. 12 μL of probes was spotted on a glass slide and the coverslip placed cell-side down onto

the droplet. Coverslips were sealed with bicycle tire glue and allowed to dry. Slides were placed in a humidity chamber containing 70% formamide, 2X SSC, sealed and place overnight at 37°C. The following morning the glue was removed and the coverslips washed off the slides by dipping them in 50% formamide, 2X SSC pH=7 at 45°C. Coverslips were washed 3X 5 min 50% formamide, 2X SSC pH=7 at 45°C, followed by 3X 5 min washes in 0.5X SSC 60°C to wash off any weakly bound probe. Coverslips were stored in PBS or immediately mounted. For biotinylated probes, coverslips were incubated with 25 μL of a 1:200 dilution of streptavidin-Cy3 (1h, RT) followed by 1:200 dilution goat anti-streptavidin-biotin (1 h, RT) with a final incubation with 25 μL 1:200 dilution of streptavidin-Cy3 (1h, RT). Coverslips were then mounted with mounting media containing Hoechst 33342 (H33342) dye as counter stain.

BAC probes for chromosome 4 (Rp11-121H14) and chromosome 19 (Rp11-79G6) were purchased from The Center for Applied Genomics (Hospital for Sick Children, University of Toronto). Each probe was directly labelled with spectrum-green dye. Probes were ethanol precipitated and suspended in hybridization buffer as described above. Hybridization and processing were conducted as for chromosome painting.



Erosion analysis was performed using an in-house developed software tool (Cell Nucleus Analyser). A minimum of 50 nuclei were analysed for chromosomes and for BAC probes. For each image this tool breaks the nucleus as defined by the H33342 staining into 5 concentric shells of equal volume; 1 being the most external and 5 being the most central. The chromosome signal is then calculated for each ring. Signals are normalized by dividing the percent chromosome signal by the percent H33342 signal present in each shell. Data is presented as a ratio and the error bars represent the standard error of the mean.

**RNA-seq data**: Changes in gene expression were derived from datasets available through the Gene Expression Omnibus, accession number GSE65145. Fold change values compared to proliferative samples were calculated as previously described **(Gillespie et al. 2015)**.

**Chromosome Conformation Capture:** Cultured cells detached from flasks using Tryple Express (ThermoFisher). Following pelleting and resuspension in 20 mL FBS-free culture media, cells were fixed in 1% formaldehyde for 10 minutes at 37°C and subsequently quenched with glycine (final concentration 155mM) for 10 min at RT. Cells were counted and pelleted at 450 X G (4°C). To permeablize the cells, the pellet was resuspended in 10 mL of 10mM Tris pH 8, 10mM NaCl and 0.1% triton-X 100 with protease inhibitors and incubated at RT for 10 min with slow mixing. Following pelleting (450 X G, 5 min 4°C) the pellet was resuspended in 1 mL for every 5 million cells present. 5 million cells were aliquoted into 1.5 mL tubes and the cells pelleted at 5,000 X G for 5 min at 4°C; 5 million cells was found to be optimal for this procedure. PBS was thoroughly drained from the cell pellet and the pellet resuspended in 50 μL of 10 mM NaCl, 10 mM Tris-HCl pH 8.0, 1 mM EDTA, 1 % SDS (3C Lysis Buffer) containing 1 X protease inhibitor cocktail. Cells were heated at 65°C for 10 min then cooled on ice for 5 min. Solution should be clear and viscous. 375 μL of $H_2O$ was added followed by 25 μL 20% v/v Triton X-100. Following mixing, 50 μL of 10 X restriction enzyme buffer (NEB 2.1) was added and the suspension mixed vigorously. 1000 U of HindIII restriction enzyme was added and the cell suspension mixed at 950 rpm (Eppendorf Thermomixer) over night at 37°C. The following morning, an additional 200 U enzyme was added and the suspension was incubated for an additional hour. 100 μL of suspension was removed to measure digestion efficiency (designated DE). To the remaining 400 μL of reaction (3C library), 80 μL of 10 X T4 DNA ligase buffer and 320 μL of water was added and followed by vigorous mixing. Chromatin was allowed to ligate at 16°C overnight with mixing at 950 rpm. To ligation reactions 40 μL 0.5 M EDTA (pH=8.0) was added along with 4 μl 100mg/ml RNAseA (Qiagen). To the DE reactions, 5 μl 0.5 M EDTA and 1 μL RNAseA was added. Reactions were incubated at 37°C for 30 min. Samples were then mixed with Proteinase K (10 μL for 3C library and 2 μL for DE sample) and incubated for 6 hours at 65°C. 400 μL H2O was the added to DE samples. At this stage both DE and 3C libraries were phenol:chloroform extracted, followed by chloroform:isoamyl (19:1) alcohol extraction and then precipitated using 2 μl (20 μg/μl) glycogen, 1/10 volume sodium acetate (3M, pH=5.2) and an equal volume isopropanol. DNA pellets were washed with ice-cold 70% ethanol and re-spun down at maximum velocity. Following drying DE samples were resuspended in 25 μL $H_2O$ and 3C libraries in 100 μL $H_2O$.

**3C primer design and validation:** PCR primer for genes/region of interest were selected to flank HindIII restriction sites in genomic DNA (**Supplemental Table 7**). All primer pairs were screened by generating a synthetic library of all 3C interactions. To test the ability of primer combinations from different pairs to detect potential 3C libraries, we created synthetic 3C libraries by first amplifying fragments of DNA containing the HindIII sites. These fragments were purified and mixed in equimolar concentrations before digestion with HindIII restriction enzyme. Following heat denaturation of the enzyme, the fragment mixture was incubated at 16$^{o}$C for 8h with T4 DNA ligase resulting in libraries of interactions of all possible fragment combinations. 10 ng of this mixture was used in qPCR reaction to determine if the possible primer pairs were acceptable for detecting unique products and thus their use in 3C reactions. All primer combinations tested were able to detect synthetic 3C products by qPCR.

**3C library quantification and normalization**: To accurately quantify the amount of DNA in each of the libraries/DE samples, we subjected 1 μL/reaction in triplicate to qPCR using primers against the *EFEMP2* gene (See **Supplemental Table 7** for a complete list of primers, sequencings, genomic locations and amplicon sizes predicted). This amplicon has no HindIII cut site between the primers and therefore was used to quantify the amount of template in each. Values obtained were compared against 50 ng of genomic DNA. Volumes of 3C and DE samples were adjusted to 50 ng/μl based on these values to obtain equal loading for subsequent analyses. DE efficiencies were measure using qPCR and comparing 50 ng of genomic DNA against 50 ng of DE sample. Therefore, a decrease in Ct values of 1 cycle would equal a 50% digestion efficiency. Libraries less the 80% digested were not carried further. As positive controls for ligation, we monitored the cutting and inversion of the *GAPDH* gene with its enhancer located in the adjacent fragment following digestion.

**Interaction strength quantification**: For each potential interaction, qPCR was performed in 10 μl reaction with 50 ng template, 300 nM forward and reverse primers (1 μl each) and 5 μl 2X qPCR mix (SYBR® Select Master Mix; Invitrogen). To normalize for the strength of interactions we chose restriction sites within the *LIF* gene (primer: *LIF* A1 3' and *LIF* A2 3'; product LIF A1XA2). This

control interaction results from 2 adjacent restriction fragments that must invert to form a detectable product. The normalization value used was applied to all other interactions identified in each library. Interaction strength is represented in relation to this value and is calculated as $2^{(40-(InteractionCT))}$; where 40 represents no detectable interaction. Error bars were calculated by using $2^{(Standard\ error\ of\ the\ mean)}$ of the measured CTs. To compare interaction strengths against proliferative values, fold change values for quiescence and rapamycin treated libraries derived above were divided by the proliferative fold change value to give the change in interaction strength as a result of treatment. T-tests indicate all values statistically significant (p-value =<0.5).

**Chromatin Immuno-precipitation:** 2DD fibroblasts were grown for 5 days in 150 mm dishes either in control media (10% FBS-containing DMEM) or treated with either 500 nM rapamycin or induced into quiescence with 0.5% FBS-containing media. The cells were fixed with 1% FA (Electron Microscopy Sciences, Cat #: 15714) in 15 mL of serum-free DMEM media for 10 min at RT. The reaction was quenched by adding glycine to a final concentration of 125 mM for 10 min at RT. Supernatant was removed and cells were washed twice in cold 1X PBS and collected by scraping in cold 1X PBS. Cells were pelleted at 200 rcf for 5 min (4°C), resuspended in 400 µl of lysis buffer (1% SDS, 10 mM EDTA, 50 mM Tris HCl ph 8.0 with 1:100 protease (Sigma-Aldrich, Cat #: P8340) and phosphatase (Sigma-Aldrich, Cat #: P5726) inhibitors) and incubated for 10 min on ice. Samples were sonicated on ice for 1 min at ~30% duty cycle, ~7% output, into chromatin fragments between 200 and 1000 bp in size. Samples were centrifuged at 12,000 rcf, 4°C for 10 min to pellet debris and supernatant transferred to new 1.5 mL tubes.

For each treatment condition, 30 µl of chromatin was used as input and 60 µl was used for each immunoprecipitation. Chromatin was quantified by Nanodrop™ spectrometer. 2.5 µg of mouse anti-rabbit anti H3K27ac (Abcam: ab4729) was added to 60 µl of chromatin, diluted 10 times in ChIP buffer (0.01% SDS, 1.1% Triton X100, 1.2 mM EDTA, 16.7 mM Tris-HCl pH 8.0 and 167 mM NaCl) containing Protease Inhibitor Cocktail 2 and Phosphatase Inhibitor Cocktail 2. 2.5 µg donkey anti-mouse HRP was used as the non-specific antibody control. Samples were incubated overnight at 4°C, rotating before binding of the samples with 50 µl of Dynabeads™ Protein A (Life Technologies, Cat #: 10006D) at 4°C for 1 h. Samples were subsequently washed for 5 minutes

three times with each of: ChIP wash buffer I (0.1% SDS, 1% Triton-X100, 2 mM EDTA, 20 mM Tris pH 8.0 and 150 mM NaCl), ChIP wash buffer II (0.1% SDS, 1% Triton X100, 2 mM EDTA, 20 mM Tris pH 8.0 and 500 mM NaCl) and ChIP wash buffer III (1 mM EDTA and 10 mM Tris-HCl pH 8.0) at RTP. Samples were eluted with 500 µL of freshly made elution buffer (1% SDS and 0.1 M NaHCO3) for 1 h at RT. For both eluted and input samples, crosslinks were reversed by adding 200 mM NaCl, 12.5 mM EDTA and 2 µL of proteinase K (Invitrogen, Cat #: 25530049) and incubating with 900 rpm agitation at 65°C for 5 h. DNA samples were extracted by phenol-chloroform extraction, adding 500 µl phenol chloroform (1:1, pH 8.0), vigorously vortexing and centrifugation (12,000 rcf for 10 min, 4°C). The upper phase was transferred to a new 1.5 mL tube and DNA precipitated by adding 2.0 µl glycogen, 1X sample volume isopropanol. Samples were then centrifuged (12,000 rcf, 30 min, 4°C) and supernatant discarded. The resultant DNA pellet from the input sample was re-suspended in 40 µL nuclease-free water and DNA from immuno-precipitated samples was re-suspended in 80 µL nuclease-free water. Chromatin shearing efficiency was monitored by running 5 µL input DNA samples on a 1.5% agarose gel. qPCR was performed in 10 µL reactions containing 5 µL PerfeCTa® SYBR® Green SuperMix for iQ (Quantabio, Cat #: 95053-500), 1 µL ChIP DNA sample, 3 µL H2O and 1 µL of 3 µM forward and reverse ChIP primers. All reactions for each gene were run in triplicate with non-template controls. ChIP-qPCR data was normalized by the percent input method.

The authors report no conflict of interest.

**Acknowledgements:**

CHE and AK are funded through the NSERC Discovery Grant Program. ZB was support by a Post-Doctoral Fellowship awarded through the College of Agriculture and Bioresources at the University of Saskatchewan. JAP and ZEG are partially supported by the Devolved Scholarship program (University of Saskatchewan). ZEG was supported by a scholarship from the Saskatchewan Innovation and Opportunity Fund. ZEG is supported by the Vanier Canada Graduate Scholarship program. JAM is funded by the Canadian Institutes of Health Research. JMB are funded through the Brunel Progeria Research Fund (UK). We would like to thank Prof. Troy

Harkness (University of Saskatchewan) for his careful reading and valuable input on this manuscript.

**Author Contributions:** JAP, ZB, and CHE performed 3C and FISH assays. AK designed and implemented strategies for linear locality clustering. ZEG assisted with bioinformatics analysis and BED graph construction. GA assisted with statistical analyses. ME developed the erosion software. JAM and JMB assisted with experimental planning and design. JAP, ZB and CHE synthesized and edited the manuscript.

Bourne, G., Moir, C., Bikkul, U., Ahmed, M.H., Kill, I.R., Eskiw, C.H., Tosi, S., and Bridger, J.M. 2013. Interphase Chromosome Behavior in Normal and Diseased Cells. 9-33.

Branco, M.R., Branco, T., Ramirez, F., and Pombo, A. 2008. Changes in chromosome organization during PHA-activation of resting human lymphocytes measured by cryo-FISH. Chromosome research : an international journal on the molecular, supramolecular and evolutionary aspects of chromosome biology *16*, 413-426.

Carter, D., Chakalova, L., Osborne, C.S., Dai, Y.F., and Fraser, P. 2002. Long-range chromatin regulatory interactions in vivo. Nature genetics *32*, 623-626.

Chambeyron, S., Da Silva, N.R., Lawson, K.A., and Bickmore, W.A. 2005. Nuclear re-organisation of the Hoxb complex during mouse embryonic development. Development *132*, 2215-2223.

Cook, P.R. (010. A model for all genomes: the role of transcription factories. J Mol Biol *395*, 1-10.

Cope, N.F., Fraser, P., and Eskiw, C. 2010. The Yin and Yang of Chromatin Spatial Organization. Genome biology *11*, 1-8.

Croft, J.A., Bridger, J.M., Boyle, S., Perry, P., Teague, P., and Bickmore, W.A. 1999. Differences in the Localization and Morphology of Chromosomes in the Human Nucleus. Journal of Cell Biology *145*, 1119-1131.

Dekker, J., Rippe, K., Dekker, M., and Kleckner, N. 2002. Capturing chromosome conformation. Science *295*, 1306-1311.

Dixon, J.R., Selvaraj, S., Yue, F., Kim, A., Li, Y., Shen, Y., Hu, M., Liu, J.S., and Ren, B. 2012. Topological domains in mammalian genomes identified by analysis of chromatin interactions. Nature *485*, 376-380.

Dostie, J., Zhan, Y., and Dekker, J. 2007. Chromosome conformation capture carbon copy technology. Curr Protoc Mol Biol *Chapter 21*, Unit 21 14.

Dottorini, T., Palladino, P., Senin, N., Persampieri, T., Spaccapelo, R., and Crisanti, A. 2013. CluGene: A Bioinformatics Framework for the Identification of Co-Localized, Co-Expressed and Co-Regulated Genes Aimed at the Investigation of Transcriptional Regulatory Networks from High-Throughput Expression Data. PloS one *8*, e66196.

Dundr, M., Ospina, J.K., Sung, M.H., John, S., Upender, M., Ried, T., Hager, G.L., and Matera, A.G. 2007. Actin-dependent intranuclear repositioning of an active gene locus in vivo. The Journal of cell biology *179*, 1095-1103.
Elcock, L.S., and Bridger, J.M. 2010. Exploring the relationship between interphase gene positioning, transcriptional regulation and the nuclear matrix. Biochemical Society transactions *38*, 263-267.
Eskiw, C.H., and Fraser, P. 2011. Ultrastructural study of transcription factories in mouse erythroblasts. J Cell Sci *124*, 3676-3683.
Eskiw, C.H., Rapp, A., Carter, D.R., and Cook, P.R. 2008. RNA polymerase II activity is located on the surface of protein-rich transcription factories. J Cell Sci *121*, 1999-2007.
Fortin, J.P., and Hansen, K.D. 2015. Reconstructing A/B compartments as revealed by Hi-C using long-range correlations in epigenetic data. Genome biology *16*, 180.
Fraser, J., Ethier, S.D., Miura, H., and Dostie, J. 2012. A Torrent of data: mapping chromatin organization using 5C and high-throughput sequencing. Methods Enzymol *513*, 113-141.
Fraser, P., and Bickmore, W. 2007. Nuclear organization of the genome and the potential for gene regulation. Nature *447*, 413-417.
Fujikawa, H., Fujimoto, A., Farooq, M., Ito, M., and Shimomura, Y. 2012. Characterization of the human hair keratin-associated protein 2 (KRTAP2) gene family. The Journal of investigative dermatology *132*, 1806-1813.
Gillespie, Z.E., MacKay, K., Sander, M., Trost, B., Dawicki, W., Wickramarathna, A., Gordon, J., Eramian, M., Kill, I.R., Bridger, J.M.*, et al.* 2015. Rapamycin reduces fibroblast proliferation without causing quiescence and induces STAT5A/B-mediated cytokine production. Nucleus, 0.
Iborra, F.J., Pombo, A., Jackson, D.A., and Cook, P.R. 1996. Active RNA polymerases are localized within discrete transcription "factories' in human nuclei. J Cell Sci *109 ( Pt 6)*, 1427-1436.
Lee, G.R., Spilianakis, C.G., and Flavell, R.A. 2005. Hypersensitive site 7 of the TH2 locus control region is essential for expressing TH2 cytokine genes and for long-range intrachromosomal interactions. Nat Immunol *6*, 42-48.
Lieberman-Aiden, E., van Berkum, N.L., Williams, L., Imakaev, M., Ragoczy, T., Telling, A., Amit, I., Lajoie, B.R., Sabo, P.J., Dorschner, M.O.*, et al.* 2009. Comprehensive mapping of long-range interactions reveals folding principles of the human genome. Science *326*, 289-293.
Mehta, I.S., Amira, M., Harvey, A.J., and Bridger, J.M. 2010. Rapid chromosome territory relocation by nuclear motor activity in response to serum removal in primary human fibroblasts. Genome biology *11*, R5.
Mehta, I.S., Eskiw, C.H., Arican, H.D., Kill, I.R., and Bridger, J.M. 2011. Farnesyltransferase inhibitor treatment restores chromosome territory positions and active chromosome dynamics in Hutchinson-Gilford progeria syndrome cells. Genome biology *12*, R74.
Mehta, I.S., Figgitt, M., Clements, C.S., Kill, I.R., and Bridger, J.M. 2007. Alterations to nuclear architecture and genome behavior in senescent cells. Ann N Y Acad Sci *1100*, 250-263.
Mitchell, J.A., Clay, I., Umlauf, D., Chen, C.Y., Moir, C.A., Eskiw, C.H., Schoenfelder, S., Chakalova, L., Nagano, T., and Fraser, P. 2012. Nuclear RNA sequencing of the mouse erythroid cell transcriptome. PloS one *7*, e49274.
Osborne, C.S., Chakalova, L., Brown, K.E., Carter, D., Horton, A., Debrand, E., Goyenechea, B., Mitchell, J.A., Lopes, S., Reik, W.*, et al.* 2004. Active genes dynamically colocalize to shared sites of ongoing transcription. Nature genetics *36*, 1065-1071.

Osborne, C.S., Chakalova, L., Mitchell, J.A., Horton, A., Wood, A.L., Bolland, D.J., Corcoran, A.E., and Fraser, P. 2007. Myc dynamically and preferentially relocates to a transcription factory occupied by Igh. PLoS biology *5*, e192.

Perez, P. 2011. Glucocorticoid receptors, epidermal homeostasis and hair follicle differentiation. Dermatoendocrinol *3*, 166-174.

Pevzner, P., and Tesler, G. 2003. Human and mouse genomic sequences reveal extensive breakpoint reuse in mammalian evolution. Proc Natl Acad Sci U S A *100*, 7672-7677.

Phillips-Cremins, J.E., Sauria, M.E., Sanyal, A., Gerasimova, T.I., Lajoie, B.R., Bell, J.S., Ong, C.T., Hookway, T.A., Guo, C., Sun, Y*., et al.* 2013. Architectural protein subclasses shape 3D organization of genomes during lineage commitment. Cell *153*, 1281-1295.

Pombo, A., Jones, E., Iborra, F.J., Kimura, H., Sugaya, K., Cook, P.R., and Jackson, D.A. 2000. Specialized transcription factories within mammalian nuclei. Crit Rev Eukaryot Gene Expr *10*, 21-29.

Schoenfelder, S., Clay, I., and Fraser, P. 2010a. The transcriptional interactome: gene expression in 3D. Current opinion in genetics & development *20*, 127-133.

Schoenfelder, S., Sexton, T., Chakalova, L., Cope, N.F., Horton, A., Andrews, S., Kurukuti, S., Mitchell, J.A., Umlauf, D., Dimitrova, D.S*., et al.* 2010b. Preferential associations between co-regulated genes reveal a transcriptional interactome in erythroid cells. Nature genetics *42*, 53-61.

Sexton, T., Bantignies, F., and Cavalli, G. 2009. Genomic interactions: chromatin loops and gene meeting points in transcriptional regulation. Semin Cell Dev Biol *20*, 849-855.

Sexton, T., Yaffe, E., Kenigsberg, E., Bantignies, F., Leblanc, B., Hoichman, M., Parrinello, H., Tanay, A., and Cavalli, G. 2012. Three-dimensional folding and functional organization principles of the Drosophila genome. Cell *148*, 458-472.

Siatecka, M., and Bieker, J.J. 2011. The multifunctional role of EKLF/KLF1 during erythropoiesis. Blood *118*, 2044-2054.

Surralles, J., Sebastian, S., and Natarajan, A.T. 1997. Chromosomes with high gene density are preferentially repaired in human cells. Mutagenesis *12*, 437-442.

Teglund, S., Olsen, A., Khan, W.N., Frangmyr, L., and Hammarstrom, S. 1994. The Pregnancy-SpecificGlycoprotein (PSG) Gene Cluster on Human Chromosome 19: Fine Structure of the 11 PSG Genes and Identification of 6 New Genes Forming a Third Subgroup within the Carcinoembryonic Antigen (CEA) Family. Genomics *23*, 669-684.

Tewari, R., Gillemans, N., Wijgerde, M., Nuez, B., von Lindern, M., Grosveld, F., and Philipsen, S. 1998. Erythroid Kru¨ ppel-like factor (EKLF) is active in primitive and definitive erythroid cells and is required for the function of 5' HS3 of the β-globin locus control region. EMBO Journal *17*, 2334-2341.

Tolhuis, B., Plalstra, R.-J., Splinter, E., Grosveld, F., and de Laat, W. 2002. Looping and interaction between hypersensitive sites in the active beta-globin locus. Molecular cell *10*, 1453–1465.

Xu, M., and Cook, P.R. 2008. Similar active genes cluster in specialized transcription factories. The Journal of cell biology *181*, 615-623.

Zhang, H., Pan, K.H., and Cohen, S.N. 2003. Senescence-specific gene expression fingerprints reveal cell-type-dependent physical clustering of up-regulated chromosomal loci. Proc Natl Acad Sci U S A *100*, 3251-3256.

Zhang, Y., McCord, R.P., Ho, Y.J., Lajoie, B.R., Hildebrand, D.G., Simon, A.C., Becker, M.S., Alt, F.W., and Dekker, J. 2012. Spatial organization of the mouse genome and its role in recurrent chromosomal translocations. Cell *148*, 908-921.
Zhou, H.Y., Katsman, Y., Dhaliwal, N.K., Davidson, S., Macpherson, N.N., Sakthidevi, M., Collura, F., and Mitchell, J.A. 2014. A Sox2 distal enhancer cluster regulates embryonic stem cell differentiation potential. Genes & development *28*, 2699-2711.
Zullo, J.M., Demarco, I.A., Pique-Regi, R., Gaffney, D.J., Epstein, C.B., Spooner, C.J., Luperchio, T.R., Bernstein, B.E., Pritchard, J.K., Reddy, K.L*., et al.* 2012. DNA sequence-dependent compartmentalization and silencing of chromatin at the nuclear lamina. Cell *149*, 1474-1487.

**Figure 1: Genes changing expression are not biased to any one chromosome.** Using RNA-seq datasets, the percent of genes from each chromosome changing >5-fold (up- and down-regulated) expression in response to quiescence (black bars) or rapamycin (grey bars) compared to proliferating fibroblasts was calculated. The percent of genes expected to change from a random distribution is also presented (white bars). Chromosome numbers are on the X-axis and the percentage range on the Y-axis. No difference greater than 2% was observed between the random list and the observed gene distributions.



**Figure 2**: **Chromosome 4 does not re-position in response to serum deprivation or rapamycin.** DNA FISH for chromosome 4 (top panel) and X (lower panel) was performed on proliferative, quiescent and rapamycin treated 2DD fibroblasts. Chromosomes are red and bulk chromatin was counterstained with H33342 (blue). Erosion analysis to determine the position of the chromosomes within the nuclear volumes was performed. The percent of the chromosome signal for each shell was divided by the percent H33342 for each shell to compensate for total chromatin content. Chromosome 4 was found pre-dominantly in shells 2 and 3 in proliferating cells (black bars) indicating an intermediate position between the nuclear periphery and the core. Quiescence induction (light grey bars) and rapamycin treatment (dark grey bars) did not induce a re-positioning of this chromosome. Labelling of the X chromosome was used as control, positioning to the periphery under all conditions. Error bars = S.E.M. Scale bar = 5μm

**Figure 3: Representative cluster of genes (Chromosome 4) including *Il-8* responds to rapamycin.** A) Quantification of RNA-seq reads generated from proliferative (Pro: blue bars; top panel), quiescence induced (Qui: red bars; middle panel) and rapamycin treated (Rap: green bars:

bottom panel) cells were up-loaded into the UCSC Genome Browser and BEDgraphs generated. BEDgraphs of chromosome 4 (74,000,000bp-75,500,000bp) encoding *Il-8, CXCL-6, CXCL-3, CXCL-2, EREG* and *AREG* was visualized, demonstrating the number of RKM normalized reads generated in the sequencing reactions. Pink caps represent transcript levels above 20. Gene locations and orientation on the chromosome is shown. B) BEDgraph peak values for each gene are listed for Pro, Qui and Rap treatments. C) Gene expression fold change values are listed for Qui and Rap treated cells compared to Pro samples.

**Figure 4: Long range chromatin interactions are strengthened in response to quiescence and rapamycin.** Using *Il-8* as the anchor, 3C libraries generated from proliferative (Pro: blue), quiescent (Qui: red) and rapamycin treated (Rap: green) probed for interactions with *CXCL-6*, *CXCL-1*, *CXCL-3* and *CXCL-2*. Grey bars highlight the regions that were probed for interactions. The relative interaction strength against a control interaction are shown on the Y-axis. Error bar = S.E.M. All interactions detected were tested by t-test and are significant to p-value =≤0.05.

**Figure 5: *LIF* interacts with putative enhancer elements enriched for H3K27ac.** Upper panel: RNA-seq reads (RKM normalized) of the region of chromosome 22 surrounding the *LIF* gene. BEDgraphs generated within the UCSC genome browser of mapped reads from proliferative 2DD fibroblasts are shown in blue, reads from quiescent induction fibroblasts in red and reads rapamycin treated cells are shown in green. Scale maximum set at 50 reads. Middle panel: regions marked by H3K27ac in seven different cell lines identified by datasets uploaded into the ENCODE database: (coloured peaks; orange – GM12878, yellow – hESC, aqua – HSMM, blue – HUVEC, purple – K562, mauve – NHEK, pink - NHLF). Using *LIF* as the anchor, 3C libraries generated from proliferative (Pro: blue), quiescent (Qui: red) and rapamycin treated (Rap: green) were probed for interactions with up-stream and down-stream genomic regions (Lower panel). HindIII cut sites within proximity to H3K27ac peaks are indicated. Grey bars highlight the regions that were probed for interactions. The relative interaction strength against a control interaction is shown in the graph. Error bar = S.E.M. All interactions detected were tested by t-test and are significant to p-value =≤0.05.

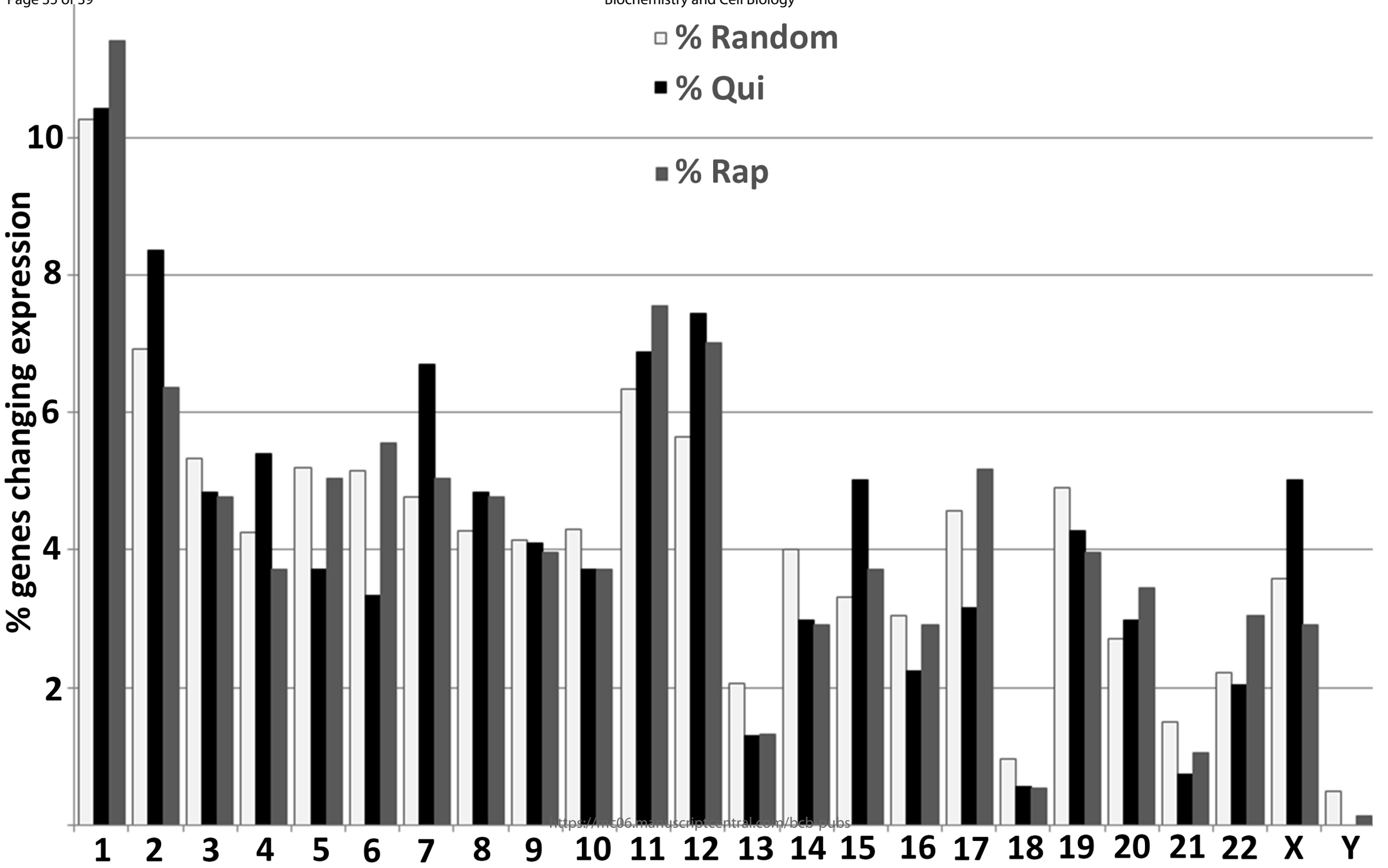

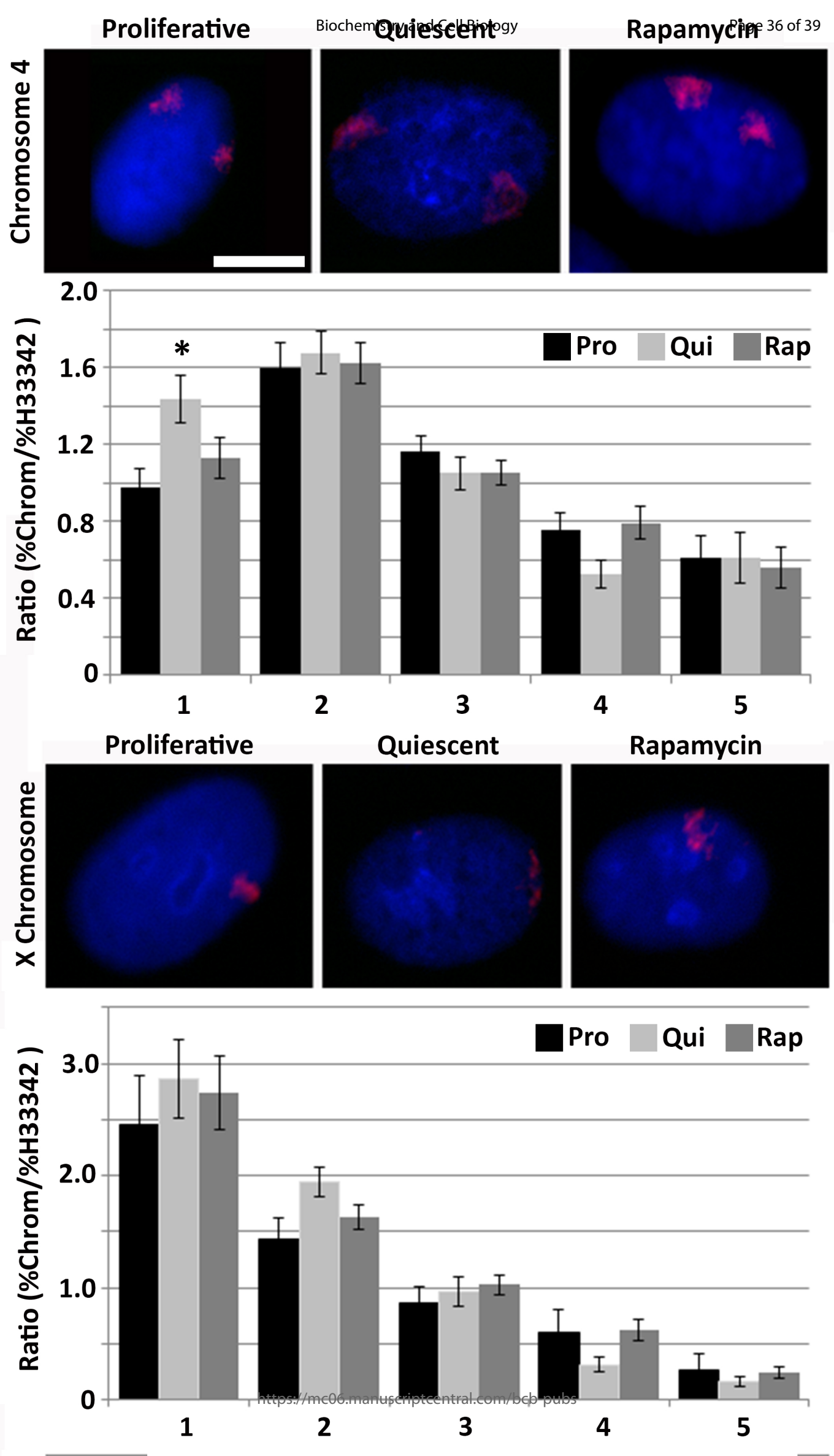

**A**

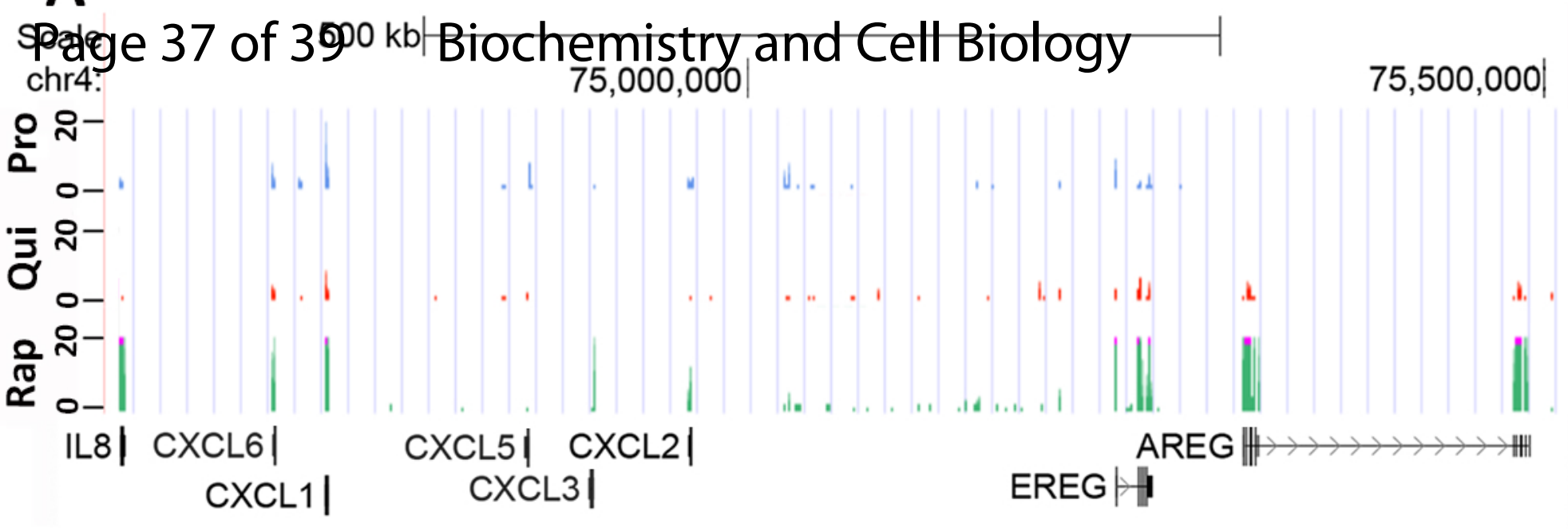


**B** BED Graph Peak Values

| | Pro | Qui | Rap |
|---|---|---|---|
| CXCL8 | 3 | 1 | 62 |
| CXCL6 | 7 | 4 | 21 |
| CXCL1 | 18 | 8 | 106 |
| CXCL5 | 7 | 2 | 1 |
| CXCL3 | 1 | 0 | 23 |
| CXCL2 | 2 | 1 | 12 |
| EREG | 8 | 6 | 77 |
| AREG | 0 | 4 | 93 |

**C** Gene Expression Fold Change Values

| | Pro | Qui | Rap |
|---|---|---|---|
| CXCL8 | 1 | -1.5 | 24.0 |
| CXCL6 | 1 | -1.4 | 3.0 |
| CXCL1 | 1 | 0.4 | 5.9 |
| CXCL5 | 1 | -1.7 | 2.3 |
| CXCL3 | 1 | -5.2 | 9.2 |
| CXCL2 | 1 | -1.8 | 5.2 |
| EREG | 1 | 1.0 | 11.3 |
| AREG | 1 | 5.9 | 81.6 |